

# Loss or Gain of Function? Ion Channel Mutation Effects on Neuronal Firing Depend on Cell Type

## **1 Abstract (250 Words Maximum - Currently 231)**

2 Ion channels determine neuronal excitability and disruption in ion channel properties in mutations  
3 can result in neurological disorders called channelopathies. Often many mutations are associated  
4 with a channelopathy, and determination of the effects of these mutations are generally done at the  
5 level of currents. The impact of such mutations on neuronal firing is vital for selecting personalized  
6 treatment plans for patients, however whether the effect of a given mutation on firing can simply be  
7 inferred from current level effects is unclear. The general impact of the ionic current environment  
8 in different neuronal types on the outcome of ion channel mutations is vital to understanding of  
9 the impacts of ion channel mutations and effective selection of personalized treatments. Using a  
10 diverse collection of neuronal models, the effects of changes in ion current properties on firing is  
11 assessed systematically and for episodic ataxia type 1 associated  $K_v1.1$  mutations. The effects of  
12 ion current property changes or mutations on firing is dependent on the current environment, or cell  
13 type, in which such a change occurs in. Characterization of ion channel mutations as loss or gain of  
14 function is useful at the level of the ionic current, however the effects of channelopathies on firing  
15 is dependent on cell type. To further the efficacy of personalized medicine in channelopathies, the  
16 effects of ion channel mutations must be examined in the context of the appropriate cell types.

## 17 **Significant Statement (120 Words Maximum - Currently 112)**

18 Ion channels determine neuronal excitability and mutations that alter ion channel properties result  
19 in neurological disorders called channelopathies. Although the genetic nature of such mutations  
20 as well as their effects on the ion channel's biophysical properties are routinely assessed exper-  
21 imentally, determination of the role in altering neuronal firing is more difficult. Computational  
22 modelling bridges this gap and demonstrates that the cell type in which a mutation occurs is an  
23 important determinant in the effects of firing. As a result, classification of ion channel mutations  
24 as loss or gain of function is useful to describe the ionic current but care should be taken when  
25 applying this classification on the level of neuronal firing.

## 26 **Introduction (750 Words Maximum - Currently 673)**

27 Neuronal ion channels are vital in determining neuronal excitability, action potential generation and  
28 firing patterns ([Bernard and Shevell, 2008](#); [Carbone and Mori, 2020](#)). In particular, the properties  
29 and combinations of ion channels and their resulting currents determine the firing properties of  
30 the neuron ([Pospischil et al., 2008](#); [Rutecki, 1992](#)). However, ion channel function can be disturb  
31 resulting in altered ionic current properties and altered neuronal firing behaviour ([Carbone and](#)  
32 [Mori, 2020](#)). Ion channel mutations are a common cause of such channelopathies and are often  
33 associated with hereditary clinical disorders ([Bernard and Shevell, 2008](#); [Carbone and Mori, 2020](#)).  
34 The effects of these mutations are frequently determined at a biophysical level, however assessment  
35 of the impact of mutations on neuronal firing and excitability is more difficult. Experimentally,  
36 transfection of cell cultures or the generation of mutant mice lines are common approaches. Cell  
37 culture transfection does not replicate the exact interplay of endogenous currents nor does it take  
38 into account the complexity of the nervous system including factors such as expression patterns,  
39 intracellular regulation and modulation of ion channels as well as network effects. Transfected

40 currents are characterized in isolation and the role of these isolated currents in the context of other  
41 currents in a neuron cannot be definitively inferred. The effects of individual currents *in vivo* also  
42 depend on the neuron type they are expressed in and which roles these neurons have in specific  
43 circuits. Complex interactions between different cell types *in vivo* are neglected in transfected cell  
44 culture. Additionally, transfected currents are not present with the neuron-type specific cellular  
45 machinery present *in vivo* and are even transfected in cells of different species. Furthermore, culture  
46 conditions can shape ion channel expression (Ponce et al., 2018).

47 Ion channel transfection of primary neuronal cultures can overcome some of the limitations of cell  
48 culture expression. In transfected neuronal cell cultures firing can more readily be assessed as en-  
49 dogenous currents are present, however the expressed and endogenous versions of the same ion  
50 channel are present in the cell (Scalmani et al., 2006; Smith et al., 2018). To avoid the confound of  
51 both expressed and endogenous current contributing to firing, a drug resistance can be introduced  
52 into the ion channel that is transfected and the drug is used to silence the endogenous version  
53 of this current (Liu et al., 2019). Although addition of TTX-resistance to Nav does not alter the  
54 gating properties of these channels (Leffler et al., 2005), the relative expression and conductance  
55 of the transfected ion channel in relation to endogenous currents can be variable and non-specific  
56 blocking of ion channels not affected by the channelopathy may occur. As the firing behaviour  
57 and dynamics of neuronal models can be dramatically altered by altering relative current ampli-  
58 tudes (Barreiro et al., 2012; Golowasch et al., 2002; Kispersky et al., 2012; Pospischil et al., 2008;  
59 Rutecki, 1992), primary neuronal cultures provide a useful general indication as to the effects of  
60 ion channel mutations but do not provide definitive insight into the effects of a channelopathy on  
61 *in vivo* firing.

62 The generation of mice lines is costly and behavioural characterization of new mice lines is required  
63 to assess similarities to patient symptoms. Although the generation of mouse lines is desirable for  
64 a clinical disorder characterized by a specific ion channel mutation, this approach becomes im-

65 practical for disorders associated with a collection of distinct mutations in a single ion channel.  
66 Because of the lack of adequate experimental approaches, a great need is present for the ability  
67 to assess the impacts of ion channel mutations on neuronal firing. A more general understand-  
68 ing of the effects of changes in current properties on neuronal firing may help to understand the  
69 impacts of ion channel mutations. Specifically, modelling approaches can be used to assess the  
70 impacts of current property changes on firing behaviour, bridging the gap between changes in the  
71 biophysical properties induced by mutations and clinical symptoms. Conductance-based neuronal  
72 models enable insight into the effects of ion channel mutations with specific effects of the resulting  
73 ionic current as well as enabling *in silico* assessment of the relative effects of changes in biophys-  
74 ical properties of ionic currents on neuronal firing. The effects of altered voltage-gated potassium  
75 channel K<sub>V</sub>1.1 function is of particular interest in this study as it gives rise to the I<sub>K<sub>V</sub>1.1</sub> current and  
76 is associated with episodic ataxia type 1. Furthermore, modelling approaches enable predictions of  
77 the effects of specific mutation and drug induced biophysical property changes.

78 K<sub>V</sub>1.1 channels, encoded by the KCNA1 gene, play a role in repolarizing the action potential, neu-  
79 ronal firing patterns, neurotransmitter release, and saltatory conduction (D'Adamo et al., 1998) and  
80 are expressed throughout the CNS (Tsaour et al., 1992; Veh et al., 1995; Wang et al., 1994). Altered  
81 K<sub>V</sub>1.1 channel function as a result of KCNA1 mutations in humans is associated with episodic  
82 ataxia type 1 (EA1) which is characterized by period attacks of ataxia and persistent myokymia  
83 (Parker, 1946; Van Dyke et al., 1975). Onset of EA1 is before 20 years of age (Brunt and van  
84 Weerden, 1990; Jen et al., 2007; Rajakulendran et al., 2007; Van Dyke et al., 1975) and is associ-  
85 ated with a 10 times higher prevalence of epileptic seizures (Zuberi et al., 1999). EA1 significantly  
86 impacts patient quality of life (Graves et al., 2014). K<sub>V</sub>1.1 null mice have spontaneous seizures  
87 without ataxia starting in the third postnatal week although impaired balance has been reported  
88 (Smart et al., 1998; Zhang et al., 1999) and neuronal hyperexcitability has been demonstrated in  
89 these mice (Brew et al., 2003; Smart et al., 1998). However, the lack of ataxia in K<sub>V</sub>1.1 null mice

90 raises the question if the hyperexcitability seen is representative of the effects of EA1 associated  
91  $K_V1.1$  mutations.

92 Using a diverse set of conductance-based neuronal models we examine the role of current environ-  
93 ment on the impact of alterations in channels properties on firing behavior generally and for EA1  
94 associated  $K_V1.1$  mutations.

## 95 **Materials and Methods**

96 All modelling and simulation was done in parallel with custom written Python 3.8 software, run on  
97 a Cent-OS 7 server with an Intel(R) Xeon (R) E5-2630 v2 CPU.

### 98 **Different Cell Models**

99 A group of neuronal models representing the major classes of cortical and thalamic neurons includ-  
100 ing regular spiking pyramidal (RS pyramidal), regular spiking inhibitory (RS inhibitory), and fast  
101 spiking (FS) cells were used (Pospischil et al., 2008). To each of these models, a  $K_V1.1$  current  
102 ( $I_{K_V1.1}$ ); (Ranjan et al., 2019) was added. A cerebellar stellate cell model from (Alexander et al.,  
103 2019) is used (Cb stellate). This model was also used with a  $K_V1.1$  current ( $I_{K_V1.1}$ ; (Ranjan et al.,  
104 2019)) in addition to the A-type potassium current (Cb stellate + $K_V1.1$ ) or replacing the A-type  
105 potassium current (Cb stellate  $\Delta K_V1.1$ ). A subthalamic nucleus neuron model as described by  
106 (Otsuka et al., 2004) are used (STN) and with a  $K_V1.1$  current ( $I_{K_V1.1}$ ; (Ranjan et al., 2019)) in  
107 addition to the A-type potassium current (STN + $K_V1.1$ ) or replacing the A-type potassium current  
108 (STN  $\Delta K_V1.1$ ). The properties and conductances of each model are detailed in Table 1 and the  
109 gating properties are unaltered from the original Cb stellate and STN models. For comparability to  
110 typical electrophysiological data fitting reported and for ease of further gating curve manipulations,

111 a Boltzmann function

$$x_{\infty} = \left( \frac{1 - a}{1 + \exp\left[\frac{V - V_{1/2}}{k}\right]} + a \right)^j \quad (1)$$

112 with slope  $k$ , voltage for half-maximal activation or inactivation ( $V_{1/2}$ ), exponent  $j$ , and persistent  
 113 current  $0 \leq a \leq 1$  were fitted for the RS pyramidal, RS inhibitory and FS models (Pospischil  
 114 et al., 2008). The properties of  $I_{K_V1.1}$  were fitted to the mean wild type biophysical parameters of  
 115  $K_V1.1$  (Lauxmann et al., 2021).

	RS Pyra- midal	RS Inhib- itory	FS	Cb Stellate	Cb Stellate + $K_V1.1$	Cb Stellate $\Delta K_V1.1$	STN	STN + $K_V1.1$	STN $\Delta K_V1.1$
$g_{Na}$	56	10	58	3.4	3.4	3.4	49	49	49
$g_K$	5.4	1.89	3.51	9.0556	8.15	9.0556	57	56.43	57
$g_{K_V1.1}$	0.6	0.21	0.39	—	0.90556	1.50159	—	0.57	0.5
$g_A$	—	—	—	15.0159	15.0159	—	5	5	—
$g_M$	0.075	0.0098	0.075	—	—	—	—	—	—
$g_L$	—	—	—	—	—	—	5	5	5
$g_T$	—	—	—	0.45045	0.45045	0.45045	5	5	5
$g_{Ca,K}$	—	—	—	—	—	—	1	1	1
$g_{Leak}$	0.0205	0.0205	0.038	0.07407	0.07407	0.07407	0.035	0.035	0.035
$\tau_{max,M}$	608	934	502	—	—	—	—	—	—
$C_m$	118.44	119.99	101.71	177.83	177.83	177.83	118.44	118.44	118.44

Table 1: Cell properties and conductances of regular spiking pyramidal neuron (RS Pyramidal), regular spiking inhibitory neuron (RS Inhibitory), fast spiking neuron (FS), cerebellar stellate cell (Cb Stellate), with additional  $I_{K_V1.1}$  (Cb Stellate  $\Delta K_V1.1$ ) and with  $I_{K_V1.1}$  replacement of  $I_A$  (Cb Stellate  $\Delta K_V1.1$ ), and subthalamic nucleus neuron (STN), with additional  $I_{K_V1.1}$  (STN  $\Delta K_V1.1$ ) and with  $I_{K_V1.1}$  replacement of  $I_A$  (STN  $K_V1.1$ ) models. All conductances are given in mS/cm<sup>2</sup>. Capacitances ( $C_m$ ) and  $\tau_{max,M}$  are given in pF and ms respectively.

	Gating	$V_{1/2}$ [mV]	$k$	$j$	$a$
	$I_{Na}$ activation	-34.33054521	-8.21450277	1.42295686	—
RS pyramidal,	$I_{Na}$ inactivation	-34.51951036	4.04059373	1	0.05
RS inhibitory,	$I_{Kd}$ activation	-63.76096946	-13.83488194	7.35347425	—
FS	$I_L$ activation	-39.03684525	-5.57756176	2.25190197	—
	$I_L$ inactivation	-57.37	20.98	1	—
	$I_M$ activation	-45	-9.9998807337	1	—
$I_{Kv1.1}$	$I_{Kv1.1}$ activation	-30.01851852	-7.73333333	1	—
	$I_{Kv1.1}$ Inactivation	-46.85851852	7.67266667	1	0.245

Table 2: For comparability to typical electrophysiological data fitting reported and for ease of further gating curve manipulations, a Boltzmann  $x_\infty = \left( \frac{1-a}{1+\exp[\frac{V-V_{1/2}}{k}]} + a \right)^j$  with slope  $k$ , voltage for half-maximal activation or inactivation ( $V_{1/2}$ ), exponent  $j$ , and persistent current  $0 \leq a \leq 1$  were fitted for the (Pospischil et al., 2008) models where  $\alpha_x$  and  $\beta_x$  are used. Gating parameters for  $I_{Kv1.1}$  are taken from (Ranjan et al., 2019) and fit to mean wild type parameters in (Lauxmann et al., 2021). Model gating not listed are taken directly from source publication.

## Firing Frequency Analysis

The membrane responses to 200 equidistant two second long current steps were simulated using the forward-Euler method with a  $\Delta t = 0.01$  ms from steady state. Current steps ranged from 0 to 1 nA for all models except for the RS inhibitory neuron models where a range of 0 to 0.35 nA was used to ensure repetitive firing across the range of input currents. For each current step, action potentials were detected as peaks with at least 50 mV prominence and a minimum interspike interval of 1 ms. The interspike interval was computed and used to determine the instantaneous firing frequencies elicited by the current step. The steady-state firing frequency were defined as the mean firing frequency in 0.5 seconds after the first action potential in the last second of the current step respectively and was used to construct frequency-current (fI) curves.

The smallest current at which steady state firing occurs was identified and the current step interval

127 preceding the occurrence of steady state firing was simulated at higher resolution (100 current  
128 steps) to determine the current at which steady state firing began. Firing was simulated with 100  
129 current steps from this current upwards for 1/5 of the overall current range. Over this range a fl  
130 curve was constructed and the integral, or area under the curve (AUC), of the fl curve over this  
131 interval was computed with the composite trapezoidal rule and used as a measure of firing rate  
132 independent from rheobase.

133 To obtain the rheobase, the current step interval preceding the occurrence of action potentials was  
134 explored at higher resolution with 100 current steps spanning the interval. Membrane responses to  
135 these current steps were then analyzed for action potentials and the rheobase was considered the  
136 lowest current step for which an action potential was elicited.

137 All models exhibit tonic firing and any instances of bursting were excluded to simplify the charac-  
138 terization of firing.

### 139 **Sensitivity Analysis and Comparison of Models**

140 Current properties of currents common to all models ( $I_{Na}$ ,  $I_K$ ,  $I_A/I_{K_V1.1}$ , and  $I_{Leak}$ ) were systemati-  
141 cally altered in a one-factor-at-a-time sensitivity analysis for all models. The gating curves for each  
142 current were shifted ( $\Delta V_{1/2}$ ) from -10 to 10 mV in increments of 1 mV. The slope ( $k$ ) of the gating  
143 curves were altered from half to twice the initial slope. Similarly, the maximal current conductance  
144 ( $g$ ) was also scaled from half to twice the initial value. For both slope and conductance alterations,  
145 alterations consisted of 21 steps spaced equally on a  $\log_2$  scale.

### 146 **Model Comparison**

Changes in rheobase ( $\Delta rheobase$ ) are calculated in relation to the original model rheobase. The  
contrast of each AUC value ( $AUC_i$ ) was computed in comparison to the AUC of the unaltered wild



type model ( $AUC_{wt}$ )

$$AUC_{contrast} = \frac{AUC_i - AUC_{wt}}{AUC_{wt}} \quad (2)$$

147 To assess whether the effects of a given alteration on  $AUC_{contrast}$  or  $\Delta rheobase$  are robust across  
148 models, the correlation between  $AUC_{contrast}$  or  $\Delta rheobase$  and the magnitude of current property  
149 alteration was computed for each alteration in each model and compared across alteration types.

150 The Kendall's  $\tau$  coefficient, a non-parametric rank correlation, is used to describe the relationship  
151 between the magnitude of the alteration and AUC or rheobase values. A Kendall  $\tau$  value of -1 or 1  
152 is indicative of monotonically decreasing and increasing relationships respectively.

### 153 **KCNA1/K<sub>V</sub>1.1 Mutations**

154 Known episodic ataxia type 1 associated KCNA1 mutations and their electrophysiological charac-  
155 terization reviewed in (Lauxmann et al., 2021). The mutation-induced changes in  $I_{K_{V1.1}}$  amplitude  
156 and activation slope ( $k$ ) were normalized to wild type measurements and changes in activation  $V_{1/2}$   
157 were used relative to wild type measurements. The effects of a mutation were also applied to  $I_A$   
158 when present as both potassium currents display prominent inactivation. In all cases, the muta-  
159 tion effects were applied to half of the  $K_{V1.1}$  or  $I_A$  under the assumption that the heterozygous  
160 mutation results in 50% of channels carrying the mutation. Frequency-current curves for each mu-  
161 tation in each model were obtained through simulation and used to characterize firing behaviour as  
162 described above. For each model the differences in mutation AUC to wild type AUC were normal-  
163 ized by wild type AUC ( $AUC_{contrast}$ ) and mutation rheobases are compared to wild type rheobase  
164 values ( $\Delta rheobase$ ). Pairwise Kendall rank correlations (Kendall  $\tau$ ) are used to compare the the  
165 correlation in the effects of  $K_{V1.1}$  mutations on AUC and rheobase between models.

## 166 **Code Accessibility**

167 The code/software described in the paper is freely available online at [URL redacted for double-  
168 blind review]. The code is available as Extended Data.

## 169 **Results**

170 To examine the role of cell specific current environments on the impact of altered ion channel  
171 properties on firing behaviour a set of neuronal models is used and properties of channels common  
172 across models are altered systematically one at a time. The effects of a set of episodic ataxia type  
173 1 associated  $K_V1.1$  mutations on firing was then examined across different neuronal models with  
174 different current environments.

### 175 **Firing Characterization**

176 Neuronal firing is a complex phenomenon and classification of firing is required for comparisons  
177 of firing across cell types and between conditions. Here we focus on the classification of two  
178 aspects of firing: rheobase (smallest injected current at which the cell fires an action potential)  
179 and the initial shape of the frequency-current (fI) curve. The quantification of the initial shape of  
180 the fI curve using by computing the area under the curve (AUC) is a measure of the initial firing at  
181 currents above rheobase (Figure 1A). The characterization of firing with AUC and rheobase enables  
182 determination of general increases or decreases in firing based on current-firing relationships, with  
183 the upper left quadrant ( $+\Delta AUC$  and  $-\Delta \text{rheobase}$ ) indicate an increase in firing, whereas the bottom  
184 right quadrant ( $-\Delta AUC$  and  $+\Delta \text{rheobase}$ ) is indicative of decreased firing (Figure 1B). In the lower  
185 left and upper right quadrants, the effects on firing are more nuance and cannot easily be described  
186 as a gain or loss of excitability.

187 Neuronal firing is heterogenous across the CNS and a set of neuronal models with heterogenous fir-  
188 ing due to different ion currents is desirable to reflect this heterogeneity. The set of neuronal models

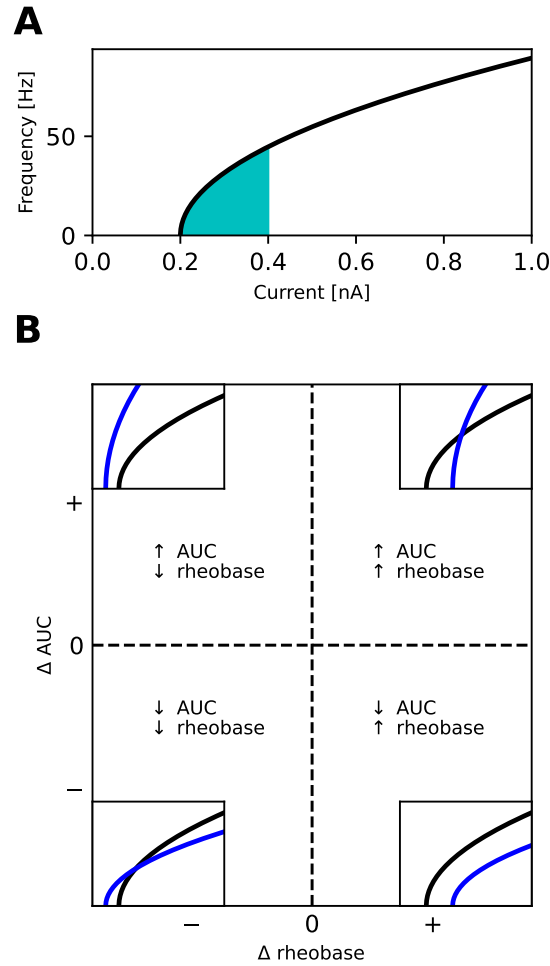


Figure 1: Characterization of firing with AUC and rheobase. (A) The area under the curve (AUC) of the repetitive firing frequency-current (fI) curve. (B) Changes in firing as characterized by  $\Delta$ AUC and  $\Delta$ rheobase occupy 4 quadrants separated by no changes in AUC and rheobase. Representative schematic fI curves in blue with respect to a reference fI curve (black) depict the general changes associated with each quadrant.

189 used here has considerable diversity as evident in the variability seen across neuronal models both  
 190 in representative spike trains and their fI curves (Figure 2). The models chosen all fire repetitively  
 191 and do not exhibit bursting. Some models, such as Cb stellate and RS inhibitory models, display  
 192 type I firing whereas others such as Cb stellate  $\Delta K_V1.1$  and STN models have type II firing. Type

193 I firing is characterized by continuous fI curve (i.e. firing rate is continuous) generated through  
 194 a saddle-node on invariant cycle bifurcation and type II firing is characterized by a discontinuity  
 195 in the fI curve (i.e. a jump occurs from no firing to firing at a certain frequency) due to a Hopf  
 196 bifurcation (Ermentrout, 1996; Ermentrout and Chow, 2002). Other models lie on a continuum  
 197 between these prototypical firing classifications. Most neuronal models exhibit hysteresis with as-  
 198 cending and descending ramps eliciting spikes with different thresholds, however STN +K<sub>V</sub>1.1 ,  
 199 STN  $\Delta$ K<sub>V</sub>1.1 , Cb stellate  $\Delta$ K<sub>V</sub>1.1 have large hysteresis (Figure 2).

## 200 Sensitivity analysis

201 Sensitivity analyses are used to understand how input model parameters contribute to the output of  
 202 a model (Saltelli, 2002). In other words, sensitivity analyses are used to understand how sensitive  
 203 the output of a model is to a change in input or model parameters. One-factor-at-a-time sensitivity  
 204 analysis involve altering one parameter at a time and enable the comparison of a given alteration in  
 205 current parameters across models. Changes in gating  $V_{1/2}$  and slope factor k as well as the current  
 206 conductance affect AUC (Figure 3 A, B and C). Heterogeneity in the correlation between gating  
 207 and conductance changes and AUC occurs across models for most currents. In these cases some of  
 208 the models display non-monotonic relationships (i.e.  $|\text{Kendall } \tau| \neq 1$ ). However, shifts in A current  
 209 activation  $V_{1/2}$ , changes in K<sub>V</sub>1.1 activation  $V_{1/2}$  and slope, and changes in A current conductance  
 210 display consistent monotonic relationships across models.

211 Alterations in gating  $V_{1/2}$  and slope factor k as well as the current conductance also play a role in  
 212 determining rheobase (Figure 4 A, B and C). Shifts in half activation of gating properties are simi-  
 213 larly correlated with rheobase across models, however Kendall  $\tau$  values departing from -1 indicate  
 214 non-monotonic relationships between K current  $V_{1/2}$  and rheobase in some models (Figure 4A).  
 215 Changes in Na current inactivation, K<sub>V</sub>1.1 current inactivation and A current activation have affect  
 216 rheobase with positive and negative correlations in different models (Figure 4B). Departures from

217 monotonic relationships occur in some models as a result of K current activation,  $K_V1.1$  current  
218 inactivation and A current activation in some models. Current conductance magnitude alterations  
219 affect rheobase similarly across models (Figure 4C).

## 220 **$K_V1.1$**

221 Mutations in  $K_V1.1$  are associated with episodic ataxia type 1 (EA1) have been characterized bio-  
222 physically and are used here as a case study in the effects of current environment on the outcomes  
223 of channelopathies on firing. The changes in AUC and rheobase from wild-type values for reported  
224 EA1 associated  $K_V1.1$  mutations are heterogenous across models containing  $K_V1.1$  , but generally  
225 show decreases in rheobase (Figure 5A-I). Pairwise non-parametric Kendall  $\tau$  rank correlations  
226 between the simulated effects of these  $K_V1.1$  mutations on rheobase are highly correlated across  
227 models (Figure 5J). However, the effects of the  $K_V1.1$  mutations on AUC are more heterogenous  
228 as reflected by both weak and strong positive and negative pairwise correlations between models  
229 (Figure 5K).

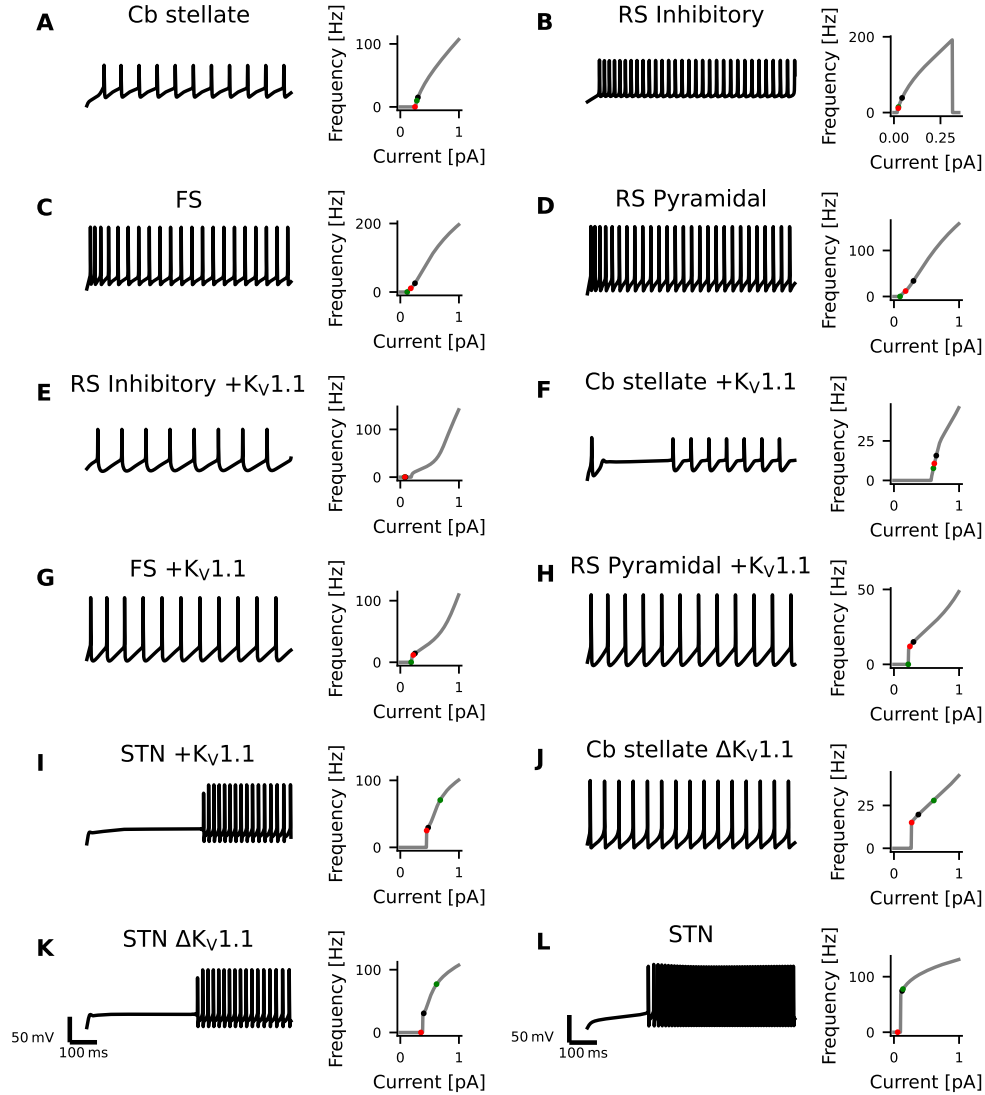


Figure 2: Diversity in Neuronal Model Firing. Spike trains (left), frequency-current (fI) curves (right) for Cb stellate (A), RS inhibitory (B), FS (C), RS pyramidal (D), RS inhibitory + $K_V1.1$  (E), Cb stellate + $K_V1.1$  (F), FS + $K_V1.1$  (G), RS pyramidal + $K_V1.1$  (H), STN + $K_V1.1$  (I), Cb stellate  $\Delta K_V1.1$  (J), STN  $\Delta K_V1.1$  (K), and STN (L) neuron models. Black marker on the fI curves indicate the current step at which the spike train occurs. The green marker indicates the current at which firing begins in response to an ascending current ramp, whereas the red marker indicates the current at which firing ceases in response to a descending current ramp (see Figure 2-1).

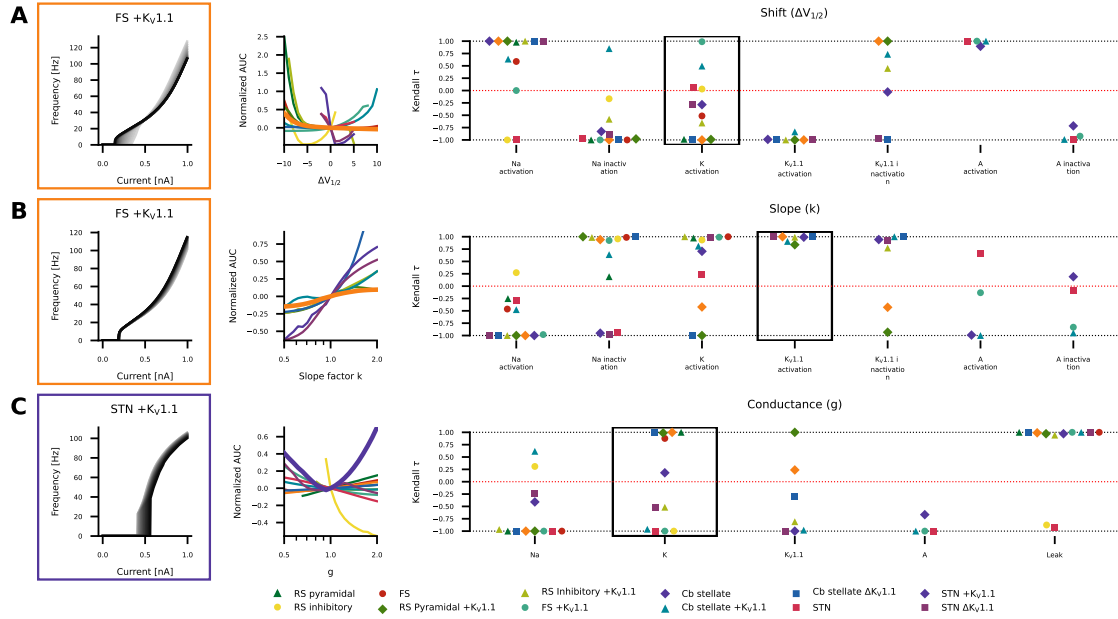


Figure 3: The Kendall rank correlation (Kendall  $\tau$ ) coefficients between shifts in  $V_{1/2}$  and AUC, slope factor k and AUC as well as current conductances and AUC for each model are shown on the right in (A), (B) and (C) respectively. The relationships between AUC and  $\Delta V_{1/2}$ , slope (k) and conductance (g) for the Kendall  $\tau$  coefficients highlights by the black box are depicted in the middle panel. The FI curves corresponding to one of the models are shown in the left panels.

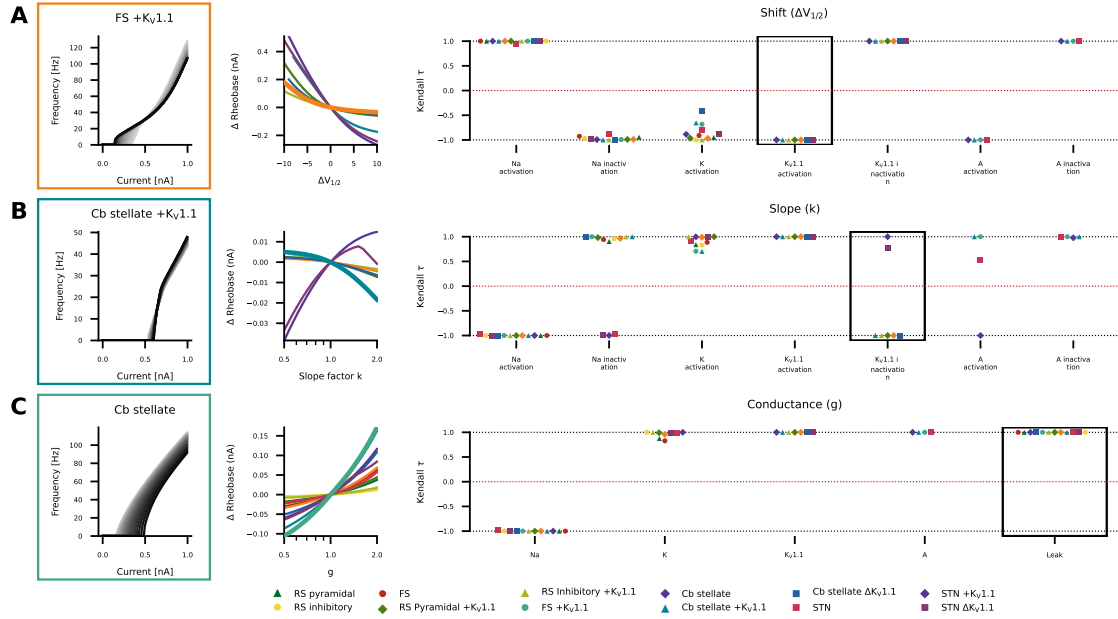


Figure 4: The Kendall rank correlation (Kendall  $\tau$ ) coefficients between shifts in  $V_{1/2}$  and rheobase, slope factor  $k$  and AUC as well as current conductances and rheobase for each model are shown on the right in (A), (B) and (C) respectively. The relationships between rheobase and  $\Delta V_{1/2}$ , slope ( $k$ ) and conductance ( $g$ ) for the Kendall  $\tau$  coefficients highlights by the black box are depicted in the middle panel. The fI curves corresponding to one of the models are shown in the left panels.



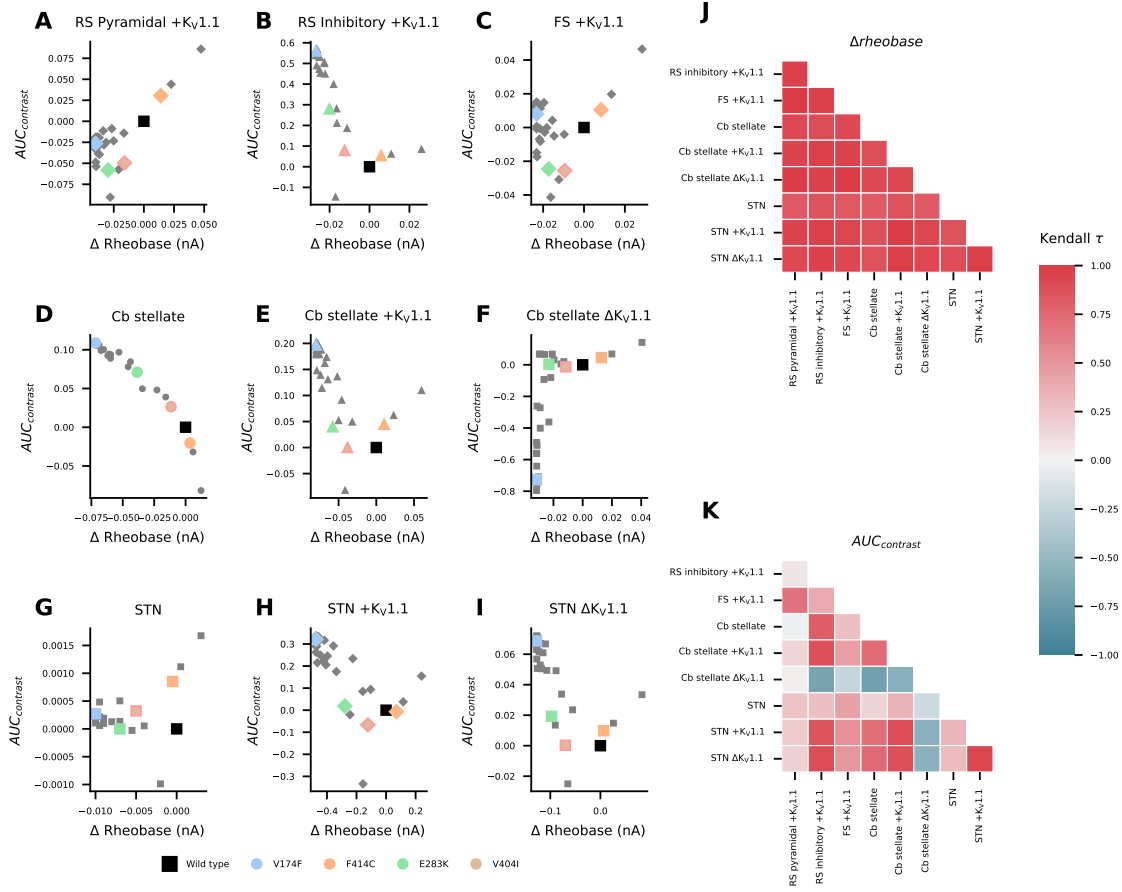


Figure 5: Effects of episodic ataxia type 1 associated  $K_V1.1$  mutations on firing. Effects of  $K_V1.1$  mutations on AUC ( $AUC_{contrast}$ ) and rheobase ( $\Delta$ rheobase) compared to wild type for RS pyramidal +  $K_V1.1$  (A), RS inhibitory +  $K_V1.1$  (B), FS +  $K_V1.1$  (C), Cb stellate (D), Cb stellate +  $K_V1.1$  (E), Cb stellate  $\Delta K_V1.1$  (F), STN (G), STN +  $K_V1.1$  (H) and STN  $\Delta K_V1.1$  (I) models V174F, F414C, E283K, and V404I mutations are highlighted in color for each model. Pair-wise Kendall rank correlation coefficients (Kendall  $\tau$ ) between the effects of  $K_V1.1$  mutations on rheobase and on AUC are shown in J and K respectively.

## Discussion (3000 Words Maximum - Currently 1780)

Using a set of diverse conductance-based neuronal models, the effects of changes to current properties and conductances on firing were determined to be heterogeneous for the AUC of the steady state fI curve but more homogeneous for rheobase. For a known channelopathy, episodic ataxia type 1 associated  $K_V1.1$  mutations, the effects on rheobase is consistent across cell types, whereas the effect on AUC is cell type dependent.

### Validity of Neuronal Models

The  $K_V1.1$  model from (Ranjan et al., 2019) is based on expression of only  $K_V1.1$  in CHO cells and represents the biophysical properties of  $K_V1.1$  homotetramers and not heteromers. Thus the  $K_V1.1$  model used here neglects the complex reality of these channels *in vivo* including their expression as heteromers and the altered biophysical properties of these heteromers (Coleman et al., 1999; Isacoff et al., 1990; Rettig et al., 1994; Roeper et al., 1998; Ruppersberg et al., 1990; Wang et al., 1999). Furthermore, dynamic modulation of  $K_V1.1$  channels, although physiologically relevant, is neglected here. For example,  $K_V\beta2$  plays a role in  $K_V1$  channel trafficking and cell membrane expression (Campomanes et al., 2002; Manganas et al., 2001; Shi et al., 2016) and  $K_V1.1$  phosphorylation increases cell membrane  $K_V1.1$  (Jonas and Kaczmarek, 1996). It should be noted that the discrete classification of potassium currents into delayed rectifier and A-type is likely not biological, but rather highlights the characteristics of a spectrum of potassium channel inactivation that arises in part due to additional factors such as heteromer composition (Glasscock, 2019; Stühmer et al., 1989), non-pore forming subunits (e.g.  $K_V\beta$  subunits) (Rettig et al., 1994; Xu and Li, 1997), and temperature (Ranjan et al., 2019) modulating channel properties.

Additionally, the single-compartment model does not take into consideration differential effects on neuronal compartments (i.e. axon, soma, dendrites), possible different spatial cellular distribution of channel expression across and within these neuronal compartments or across CNS regions nor

254 does it consider different channel types (e.g  $\text{Na}_V1.1$  vs  $\text{Na}_V1.8$ ). More realistic models would con-  
255 sist of multiple compartments, take more currents into account and take the spatial distribution of  
256 channels into account, however these models are more computationally expensive, require current  
257 specific models and knowledge of the distribution of conductances across the cell. Despite these  
258 limitations, each of the models can reproduce physiological firing behaviour of the neurons they  
259 represent (Alexander et al., 2019; Otsuka et al., 2004; Pospischil et al., 2008) and capture key as-  
260 pects of the dynamics of these cell types. The firing characterization was performed on adapted  
261 firing and as such currents that cause adaptation are neglected in our analysis.

## 262 **Current Environments Determine the Effect of Ion Channel Mutations**

263 One-factor-at-a-time (OFAT) sensitivity analyses such as the one performed here are predicated  
264 on assumptions of model linearity, and cannot account for interactions between factors (Czitrom,  
265 1999; Saltelli and Annoni, 2010). OFAT approaches are local and not global (i.e. always in refer-  
266 ence to a baseline point in the parameter space) and therefore cannot be generalized to the global  
267 parameter space unless linearity is met (Saltelli and Annoni, 2010). The local space around the  
268 wild type neuron is explored with an OFAT sensitivity analysis without taking interactions be-  
269 tween parameters into account. Comparisons between the effects of changes in similar parameters  
270 across different models can be made at the wild type locale indicative of experimentally observed  
271 neuronal behaviour. In this case, the role of deviations in the ionic current properties from their  
272 wild type in multiple neuronal models presented here provides a starting point for understanding  
273 the general role of these current properties in neurons. However, a more global approach would  
274 provide a more holistic understanding of the parameter space and provide insight into interactions  
275 between properties.

276 Characterization of the effects of a parameter on firing with non-parametric Kendall  $\tau$  correlations  
277 takes into account the sign and monotonicity of the correlation. In other words Kendall  $\tau$  coeffi-

278 cients provide information as to whether changing a parameter is positively or negatively correlated  
279 with AUC or rheobase as well as the extent to which this correlation is positive or negative across  
280 the parameter range examined. Therefore, Kendall  $\tau$  coefficients provide general information as to  
281 the sensitivity of different models to a change in a given current property, however more nuanced  
282 difference between the sensitivities of models to current property changes, such as the slope of the  
283 relationship between parameter change and firing are not included in our analysis.

284 Although, to our knowledge, no comprehensive evaluation of how current environment and cell  
285 type affect the outcome of ion channel mutations, comparisons between the effects of such mu-  
286 tations in certain cells have been reported. For instance, mutations in the SCN1A gene encoding  
287 Nav1.1 result in epileptic phenotypes by selective hypoexcitability of inhibitory but not excitatory  
288 neurons in the cortex resulting in circuit hyperexcitability ([Hedrich et al., 2014](#)). In CA3 of the hip-  
289 pocampus, mutation of Nav1.6 similarly results in increased excitability of pyramidal neurons and  
290 decreased excitability of parvalbumin positive interneurons ([Makinson et al., 2016](#)). Additionally,  
291 the L858H mutation in Nav1.7, associated with erythromyalgia, has been shown to cause hypox-  
292 citability in sympathetic ganglion neurons and hyperexcitability in dorsal root ganglion neurons  
293 ([Rush et al., 2006](#); [Waxman, 2007](#)). The differential effects of L858H Nav1.7 on firing is depen-  
294 dent on the presence or absence of another sodium channel Nav1.8 ([Rush et al., 2006](#); [Waxman,](#)  
295 [2007](#)). In a modelling study, it was found that altering the sodium conductance in 2 stomatogastric  
296 ganglion neuron models from a population models decreases rheobase in both models, however  
297 the initial slope of the fI curves (proportional to AUC) is increased in one model and decreased  
298 in the other suggesting that the magnitude of other currents in these models (such as  $K_d$ ) deter-  
299 mines the effect of a change in sodium current ([Kispersky et al., 2012](#)). These findings, in concert  
300 with our findings suggest that the current environment in which a channelopathy occurs is vital in  
301 determining the outcomes of the channelopathy on firing.

302 Cell type specific differences in current properties are important in the effects of ion channel mu-

tations, however within a cell type heterogeneity in channel expression levels exists and it is often desirable to generate a population of neuronal models and to screen them for plausibility to biological data in order to capture neuronal population diversity (Marder and Taylor, 2011). The models we used here are originally generated by characterization of current gating properties and by fitting of maximal conductances to experimental data (Alexander et al., 2019; Otsuka et al., 2004; Pospischil et al., 2008; Ranjan et al., 2019). This practice of fixing maximal conductances based on experimental data is limiting as it does not reproduce the variability in channel expression and neuronal firing behaviour of a heterogeneous neuron population (Verma et al., 2020). For example, a model derived from the mean conductances in a sub-population of stomatogastric ganglion "one-spike bursting" neurons fires 3 spikes instead of 1 per burst due to an L shaped distribution of sodium and potassium conductances (Golowasch et al., 2002). Multiple sets of current conductances can give rise to the same patterns of activity also termed degeneracy and differences in neuronal dynamics may only be evident with perturbations (Goaillard and Marder, 2021; Marder and Taylor, 2011). Variability in ion channel expression often correlates with the expression of other ion channels (Goaillard and Marder, 2021) and neurons whose behaviour is similar may possess correlated variability across different ion channels resulting in stability in neuronal phenotype (Lamb and Calabrese, 2013; Soofi et al., 2012; Taylor et al., 2009). The variability of ion currents and degeneracy of neurons may account, at least in part, for the observation that the effect of toxins within a neuronal type is frequently not constant (Khaliq and Raman, 2006; Puopolo et al., 2007; Ransdell et al., 2013).

### Effects of KCNA1 Mutations

Moderate changes in delayed rectifier potassium currents change the bifurcation structure of Hodgkin Huxley model, with changes analogous to those seen with  $K_V1.1$  mutations resulting in increased excitability due to reduced thresholds for repetitive firing (Hafez and Gottschalk, 2020). Although the Hodgkin Huxley delayed rectifier lacks inactivation, the increases in excitability seen

are in line with both score-based and simulation-based predictions of the outcomes of *KCNA1* mutations. LOF *KCNA1* mutations generally increase neuronal excitability, however the different effects of *KCNA1* mutations across models on AUC are indicative that a certain cell type specific complexity exists. Increased excitability seen experimentally with  $K_V1.1$  null mice (Smart et al., 1998; Zhou et al., 1998), with pharmacological  $K_V1.1$  block (Chi and Nicol, 2007; Morales-Villagrán et al., 1996), by (Hafez and Gottschalk, 2020) and with simulation-based predictions of *KCNA1* mutations. Contrary to these results, (Zhao et al., 2020) predicted *in silico* that the depolarizing shifts seen as a result of *KCNA1* mutations broaden action potentials and interfere negatively with high frequency action potential firing, however comparability of firing rates is lacking in this study. Different current properties, such as the difference in  $I_A$  and  $I_{K_V1.1}$  in the Cb stellate and STN model families alter the impact of *KCNA1* mutations on firing highlighting that knowledge of the biophysical properties of a current and its neuronal expression is vital for holistic understanding of the effects of a given ion channel mutation both at a single cell and network level.

## **Loss or Gain of Function Characterizations Do Not Fully Capture Ion Channel Mutation Effects on Firing**

The effects of changes in current properties depend in part on the neuronal model in which they occur and can be seen in the variance of correlations (especially in AUC) across models for a given current property change. Therefore, relative conductances and gating properties of currents in the current environment in which an alteration in current properties occurs plays an important role in determining the outcome on firing. The use of loss of function (LOF) and gain of function (GOF) is useful at the level of ion channels and whether a mutation results in more or less ionic current, however the extension of this thinking onto whether mutations induce LOF or GOF at the level of neuronal firing based on the ionic current LOF/GOF is problematic due to the dependency of neuronal firing changes on the current environment. Thus the direct leap from current level LOF/GOF characterizations to effects on firing without experimental or modelling-based evidence, although

tempting, should be refrained from and viewed with caution when reported. This is especially relevant in the recent development of personalized medicine for channelopathies, where a patients specific channelopathy is identified and used to tailor treatments (Ackerman et al., 2013; Gnecchi et al., 2021; Helbig and Ellis, 2020; Weber et al., 2017). However, the effects of specific ion channel mutations are often characterized in expression systems and classified as LOF or GOF to aid in treatment decisions (Brunklaus et al., 2022; Johannesen et al., 2021; Musto et al., 2020). Interestingly, both LOF and GOF  $\text{Na}_V1.1$  mutations can benefit from treatment with sodium channel blockers (Johannesen et al., 2021), suggesting that the relationship between effects at the level of ion channels and effects at the level of firing and therapeutics is not linear or evident without further contextual information. Therefore, this approach must be used with caution and the cell type which expressed the mutant ion channel must be taken into account. Experimental assessment of the effects of a patients specific ion channel mutation *in vivo* is not feasible at a large scale due to time and cost constraints, modelling of the effects of patient specific channelopathies is a desirable approach. Accordingly, for accurate modelling and predictions of the effects of mutations on neuronal firing, information as to the type of neurons containing the affected channel, and the properties of the affected and all currents in the affected neuronal type is needed. When modelling approaches are sought out to overcome the limitations of experimental approaches, care must be taken to account for model dependency and the generation of relevant cell-type or cell specific populations of models should be standard in assessing the effects of mutations in specific neurons.

## References

- Ackerman, M. J., Marcou, C. A. and Tester, D. J. (2013), ‘Personalized Medicine: Genetic Diagnosis for Inherited Cardiomyopathies/Channelopathies’, *Revista Española de Cardiología (English Edition)* **66**(4), 298–307.  
**URL:** <https://www.sciencedirect.com/science/article/pii/S1885585713000376>
- Alexander, R. P. D., Mitry, J., Sareen, V., Khadra, A. and Bowie, D. (2019), ‘Cerebellar Stellate

- 378 Cell Excitability Is Coordinated by Shifts in the Gating Behavior of Voltage-Gated Na<sup>+</sup> and A-  
379 Type K<sup>+</sup> Channels', *eNeuro* **6**(3).  
380 **URL:** <https://www.eneuro.org/content/6/3/ENEURO.0126-19.2019>
- 381 Barreiro, A. K., Thilo, E. L. and Shea-Brown, E. (2012), 'A-current and type I/type II transition  
382 determine collective spiking from common input', *Journal of Neurophysiology* **108**(6), 1631–  
383 1645.  
384 **URL:** <https://www.ncbi.nlm.nih.gov/pmc/articles/PMC3544951/>
- 385 Bernard, G. and Shevell, M. I. (2008), 'Channelopathies: A Review', *Pediatric Neurology*  
386 **38**(2), 73–85.  
387 **URL:** <https://www.sciencedirect.com/science/article/pii/S0887899407004584>
- 388 Brew, H. M., Hallows, J. L. and Tempel, B. L. (2003), 'Hyperexcitability and reduced low threshold  
389 potassium currents in auditory neurons of mice lacking the channel subunit Kv1.1', *The Journal*  
390 *of Physiology* **548**(1), 1–20.  
391 **URL:** <https://physoc.onlinelibrary.wiley.com/doi/abs/10.1111/j.2003.t01-1-00001.x>
- 392 Brunklaus, A., Feng, T., Brünger, T., Perez-Palma, E., Heyne, H., Matthews, E., Semsarian, C.,  
393 Symonds, J. D., Zuberi, S. M., Lal, D. and Schorge, S. (2022), 'Gene variant effects across  
394 sodium channelopathies predict function and guide precision therapy', *Brain* p. awac006.  
395 **URL:** <https://doi.org/10.1093/brain/awac006>
- 396 Brunt, E. R. P. and van Weerden, T. W. (1990), 'Familial Paroxysmal Kinesigenic Ataxia and  
397 Continuous Myokymia', *Brain* **113**(5), 1361–1382.  
398 **URL:** <https://doi.org/10.1093/brain/113.5.1361>
- 399 Campomanes, C. R., Carroll, K. I., Manganas, L. N., Hershberger, M. E., Gong, B., Antonucci,  
400 D. E., Rhodes, K. J. and Trimmer, J. S. (2002), 'Kv $\beta$  Subunit Oxidoreductase Activity and Kv1  
401 Potassium Channel Trafficking', *Journal of Biological Chemistry* **277**(10), 8298–8305.  
402 **URL:** <https://www.sciencedirect.com/science/article/pii/S0021925819364324>
- 403 Carbone, E. and Mori, Y. (2020), 'Ion channelopathies to bridge molecular lesions, channel func-  
404 tion, and clinical therapies', *Pflügers Archiv - European Journal of Physiology* **472**(7), 733–738.  
405 **URL:** <https://doi.org/10.1007/s00424-020-02424-y>
- 406 Chi, X. X. and Nicol, G. D. (2007), 'Manipulation of the Potassium Channel Kv1.1 and Its Effect  
407 on Neuronal Excitability in Rat Sensory Neurons', *Journal of Neurophysiology* **98**(5), 2683–  
408 2692.  
409 **URL:** <https://journals.physiology.org/doi/full/10.1152/jn.00437.2007>
- 410 Coleman, S. K., Newcombe, J., Pryke, J. and Dolly, J. O. (1999), 'Subunit Composition of Kv1  
411 Channels in Human CNS', *Journal of Neurochemistry* **73**(2), 849–858.  
412 **URL:** <https://onlinelibrary.wiley.com/doi/abs/10.1046/j.1471-4159.1999.0730849.x>



- 413 Czitrom, V. (1999), ‘One-Factor-at-a-Time versus Designed Experiments’, *The American Statisti-*  
 414 *cian* **53**(2), 126–131.  
 415 **URL:** <https://www.jstor.org/stable/2685731>
- 416 D’Adamo, M. C., Liu, Z., Adelman, J. P., Maylie, J. and Pessia, M. (1998), ‘Episodic ataxia type-1  
 417 mutations in the hKv1.1 cytoplasmic pore region alter the gating properties of the channel’, *The*  
 418 *EMBO Journal* **17**(5), 1200–1207.  
 419 **URL:** <https://www.embopress.org/doi/full/10.1093/emboj/17.5.1200>
- 420 Ermentrout, B. (1996), ‘Type I Membranes, Phase Resetting Curves, and Synchrony’,  
 421 *Neural Computation* **8**(5), 979–1001. \_eprint: [https://direct.mit.edu/neco/article-](https://direct.mit.edu/neco/article-pdf/8/5/979/813352/neco.1996.8.5.979.pdf)  
 422 [pdf/8/5/979/813352/neco.1996.8.5.979.pdf](https://direct.mit.edu/neco/article-pdf/8/5/979/813352/neco.1996.8.5.979.pdf).  
 423 **URL:** <https://doi.org/10.1162/neco.1996.8.5.979>
- 424 Ermentrout, G. and Chow, C. C. (2002), ‘Modeling neural oscillations’, *Physiology & Behavior*  
 425 **77**(4), 629–633.  
 426 **URL:** <https://www.sciencedirect.com/science/article/pii/S0031938402008983>
- 427 Glasscock, E. (2019), ‘Kv1.1 channel subunits in the control of neurocardiac function’, *Channels*  
 428 **13**(1), 299–307.  
 429 **URL:** <https://doi.org/10.1080/19336950.2019.1635864>
- 430 Gneccchi, M., Sala, L. and Schwartz, P. J. (2021), ‘Precision Medicine and cardiac channelopathies:  
 431 when dreams meet reality’, *European Heart Journal* **42**(17), 1661–1675.  
 432 **URL:** <https://doi.org/10.1093/eurheartj/ehab007>
- 433 Goaillard, J.-M. and Marder, E. (2021), ‘Ion Channel Degeneracy, Variability, and Covariation in  
 434 Neuron and Circuit Resilience’, *Annual Review of Neuroscience* .  
 435 **URL:** <https://www.annualreviews.org/doi/10.1146/annurev-neuro-092920-121538>
- 436 Golowasch, J., Goldman, M. S., Abbott, L. F. and Marder, E. (2002), ‘Failure of Averaging in the  
 437 Construction of a Conductance-Based Neuron Model’, *Journal of Neurophysiology* **87**(2), 1129–  
 438 1131.  
 439 **URL:** <https://journals.physiology.org/doi/full/10.1152/jn.00412.2001>
- 440 Graves, T. D., Cha, Y.-H., Hahn, A. F., Barohn, R., Salajegheh, M. K., Griggs, R. C., Bundy,  
 441 B. N., Jen, J. C., Baloh, R. W., Hanna, M. G. and on behalf of the CINCH Investigators (2014),  
 442 ‘Episodic ataxia type 1: clinical characterization, quality of life and genotype–phenotype corre-
- 443 *lation*’, *Brain* **137**(4), 1009–1018.  
 444 **URL:** <https://doi.org/10.1093/brain/awu012>
- 445 Hafez, O. A. and Gottschalk, A. (2020), ‘Altered neuronal excitability in a Hodgkin-Huxley model  
 446 incorporating channelopathies of the delayed rectifier potassium channel’, *Journal of Computa-*  
 447 *tional Neuroscience* **48**(4), 377–386.  
 448 **URL:** <https://doi.org/10.1007/s10827-020-00766-1>

- 449 Hedrich, U. B., Liautard, C., Kirschenbaum, D., Pofahl, M., Lavigne, J., Liu, Y., Theiss, S., Slotta,  
450 J., Escayg, A., Dihné, M., Beck, H., Mantegazza, M. and Lerche, H. (2014), ‘Impaired action po-  
451 tential initiation in gabaergic interneurons causes hyperexcitable networks in an epileptic mouse  
452 model carrying a human nav1.1 mutation’, *Journal of Neuroscience* **34**(45), 14874–14889.  
453 **URL:** <https://www.jneurosci.org/content/34/45/14874>
- 454 Helbig, I. and Ellis, C. A. (2020), ‘Personalized medicine in genetic epilepsies – possibilities,  
455 challenges, and new frontiers’, *Neuropharmacology* **172**, 107970.  
456 **URL:** <https://www.sciencedirect.com/science/article/pii/S0028390820300368>
- 457 Isacoff, E. Y., Jan, Y. N. and Jan, L. Y. (1990), ‘Evidence for the formation of heteromultimeric  
458 potassium channels in *Xenopus* oocytes’, *Nature* **345**(6275), 530–534.  
459 **URL:** <https://www.nature.com/articles/345530a0>
- 460 Jen, J., Graves, T., Hess, E., Hanna, M., Griggs, R., Baloh, R. and the CINCH investigators (2007),  
461 ‘Primary episodic ataxias: diagnosis, pathogenesis and treatment’, *Brain* **130**(10), 2484–2493.  
462 **URL:** <https://doi.org/10.1093/brain/awm126>
- 463 Johannesen, K. M., Liu, Y., Gjerulfsen, C. E., Koko, M., Sonnenberg, L., Schubert, J., Fenger,  
464 C. D., Eltokhi, A., Rannap, M., Koch, N. A., Lauxmann, S., Krüger, J., Kegele, J., Canafoglia,  
465 L., Franceschetti, S., Mayer, T., Rebstock, J., Zacher, P., Ruf, S., Alber, M., Sterbova, K., Las-  
466 suthová, P., Vlckova, M., Lemke, J. R., Krey, I., Heine, C., Wiczorek, D., Kroell-Seger, J.,  
467 Lund, C., Klein, K. M., Au, P. B., Rho, J. M., Ho, A. W., Masnada, S., Veggiotti, P., Giordano,  
468 L., Accorsi, P., Hoei-Hansen, C. E., Striano, P., Zara, F., Verhelst, H., S.Verhoeven, J., Zwaag, B.  
469 v. d., Harder, A. V. E., Brilstra, E., Pendziwiat, M., Lebon, S., Vaccarezza, M., Le, N. M., Chris-  
470 tensen, J., Schmidt-Petersen, M. U., Grønborg, S., Scherer, S. W., Howe, J., Fazeli, W., Howell,  
471 K. B., Leventer, R., Stutterd, C., Walsh, S., Gerard, M., Gerard, B., Matricardi, S., Bonardi,  
472 C. M., Sartori, S., Berger, A., Hoffman-Zacharska, D., Mastrangelo, M., Darra, F., Vølle, A.,  
473 Motazacker, M. M., Lakeman, P., Nizon, M., Betzler, C., Altuzarra, C., Caume, R., Roubertie,  
474 A., Gélisse, P., Marini, C., Guerrini, R., Bilan, F., Tibussek, D., Koch-Hogrebe, M., Perry, M. S.,  
475 Ichikawa, S., Dadali, E., Sharkov, A., Mishina, I., Abramov, M., Kanivets, I., Korostelev, S., Kut-  
476 sev, S., Wain, K. E., Eisenhauer, N., Wagner, M., Savatt, J. M., Müller-Schlüter, K., Bassan, H.,  
477 Borovikov, A., Nassogne, M.-C., Destrée, A., Schoonjans, A.-S., Meuwissen, M., Buzatu, M.,  
478 Jansen, A., Scalais, E., Srivastava, S., Tan, W.-H., Olson, H. E., Loddenkemper, T., Poduri, A.,  
479 Helbig, K. L., Helbig, I., Fitzgerald, M. P., Goldberg, E. M., Roser, T., Borggraefe, I., Brünger,  
480 T., May, P., Lal, D., Lederer, D., Rubboli, G., Lesca, G., Hedrich, U. B., Benda, J., Gardella,  
481 E., Lerche, H. and Møller, R. S. (2021), ‘Genotype-phenotype correlations in SCN8A-related  
482 disorders reveal prognostic and therapeutic implications’, *medRxiv* p. 2021.03.22.21253711.  
483 **URL:** <https://www.medrxiv.org/content/10.1101/2021.03.22.21253711v1>
- 484 Jonas, E. A. and Kaczmarek, L. K. (1996), ‘Regulation of potassium channels by protein kinases’,  
485 *Current Opinion in Neurobiology* **6**(3), 318–323.  
486 **URL:** <https://www.sciencedirect.com/science/article/pii/S0959438896801140>

- 487 Khaliq, Z. M. and Raman, I. M. (2006), 'Relative Contributions of Axonal and Somatic Na Chan-  
488 nels to Action Potential Initiation in Cerebellar Purkinje Neurons', *Journal of Neuroscience*  
489 **26**(7), 1935–1944.
- 490 Kispersky, T. J., Caplan, J. S. and Marder, E. (2012), 'Increase in Sodium Conductance Decreases  
491 Firing Rate and Gain in Model Neurons', *Journal of Neuroscience* **32**(32), 10995–11004.  
492 **URL:** <https://www.jneurosci.org/content/32/32/10995>
- 493 Lamb, D. G. and Calabrese, R. L. (2013), 'Correlated Conductance Parameters in Leech Heart  
494 Motor Neurons Contribute to Motor Pattern Formation', *PLOS ONE* **8**(11), e79267.  
495 **URL:** <https://journals.plos.org/plosone/article?id=10.1371/journal.pone.0079267>
- 496 Lauxmann, S., Sonnenberg, L., Koch, N. A., Boßelmann, C. M., Winter, N., Schwarz, N., Wuttke,  
497 T. V., Hedrich, U. B. S., Liu, Y., Lerche, H., Benda, J. and Kegele, J. (2021), 'Therapeutic po-  
498 tential of sodium channel blockers as targeted therapy approach in KCNA1-associated episodic  
499 ataxia (EA1) and a comprehensive review of the literature', *Frontiers in Neurology* **In Press**.  
500 **URL:** <https://www.frontiersin.org/articles/10.3389/fneur.2021.703970/abstract>
- 501 Leffler, A., Herzog, R. I., Dib-Hajj, S. D., Waxman, S. G. and Cummins, T. R. (2005), 'Pharma-  
502 cological properties of neuronal TTX-resistant sodium channels and the role of a critical serine  
503 pore residue', *Pflügers Archiv* **451**(3), 454–463.  
504 **URL:** <https://doi.org/10.1007/s00424-005-1463-x>
- 505 Liu, Y., Schubert, J., Sonnenberg, L., Helbig, K. L., Hoei-Hansen, C. E., Koko, M., Rannap, M.,  
506 Lauxmann, S., Huq, M., Schneider, M. C., Johannesen, K. M., Kurlermann, G., Gardella, E.,  
507 Becker, F., Weber, Y. G., Benda, J., Møller, R. S. and Lerche, H. (2019), 'Neuronal mechanisms  
508 of mutations in SCN8A causing epilepsy or intellectual disability', *Brain* **142**(2), 376–390.  
509 **URL:** <https://doi.org/10.1093/brain/awy326>
- 510 Makinson, C. D., Dutt, K., Lin, F., Papale, L. A., Shankar, A., Barela, A. J., Liu, R., Goldin, A. L.  
511 and Escayg, A. (2016), 'An Scn1a epilepsy mutation in Scn8a alters seizure susceptibility and  
512 behavior', *Experimental Neurology* **275**, 46–58.  
513 **URL:** <https://www.sciencedirect.com/science/article/pii/S001448861530090X>
- 514 Manganas, L. N., Wang, Q., Scannevin, R. H., Antonucci, D. E., Rhodes, K. J. and Trimmer, J. S.  
515 (2001), 'Identification of a trafficking determinant localized to the Kv1 potassium channel pore',  
516 *Proceedings of the National Academy of Sciences* **98**(24), 14055–14059.  
517 **URL:** <https://www.pnas.org/content/98/24/14055>
- 518 Marder, E. and Taylor, A. L. (2011), 'Multiple models to capture the variability in biological neu-  
519 rons and networks', *Nature Neuroscience* **14**(2), 133–138.  
520 **URL:** <https://www.nature.com/articles/nn.2735>
- 521 Morales-Villagrán, A., Ureña-Guerrero, M. E. and Tapia, R. (1996), 'Protection by NMDA re-  
522 ceptor antagonists against seizures induced by intracerebral administration of 4-aminopyridine',

- 523 *European Journal of Pharmacology* **305**(1), 87–93.  
 524 **URL:** <https://www.sciencedirect.com/science/article/pii/S0014299996001574>
- 525 Musto, E., Gardella, E. and Møller, R. S. (2020), ‘Recent advances in treatment of epilepsy-related  
 526 sodium channelopathies’, *European Journal of Paediatric Neurology* **24**, 123–128.  
 527 **URL:** <https://www.sciencedirect.com/science/article/pii/S1090379819304295>
- 528 Otsuka, T., Abe, T., Tsukagawa, T. and Song, W.-J. (2004), ‘Conductance-Based Model of the  
 529 Voltage-Dependent Generation of a Plateau Potential in Subthalamic Neurons’, *Journal of Neu-*  
 530 *rophysiology* **92**(1), 255–264.  
 531 **URL:** <https://journals.physiology.org/doi/full/10.1152/jn.00508.2003>
- 532 Parker, H. L. (1946), ‘Periodic ataxia’, *Collected Papers of the Mayo Clinic and the Mayo Foun-*  
 533 *dedation. Mayo Clinic* **38**, 642–645.
- 534 Ponce, A., Castillo, A., Hinojosa, L., Martinez-Rendon, J. and Cereijido, M. (2018), ‘The expres-  
 535 sion of endogenous voltage-gated potassium channels in HEK293 cells is affected by culture  
 536 conditions’, *Physiological Reports* **6**(8), e13663.  
 537 **URL:** <https://www.ncbi.nlm.nih.gov/pmc/articles/PMC5903699/>
- 538 Pospischil, M., Toledo-Rodriguez, M., Monier, C., Piwkowska, Z., Bal, T., Frégnac, Y., Markram,  
 539 H. and Destexhe, A. (2008), ‘Minimal Hodgkin–Huxley type models for different classes of  
 540 cortical and thalamic neurons’, *Biological Cybernetics* **99**(4), 427–441.  
 541 **URL:** <https://doi.org/10.1007/s00422-008-0263-8>
- 542 Puopolo, M., Raviola, E. and Bean, B. P. (2007), ‘Roles of Subthreshold Calcium Current and  
 543 Sodium Current in Spontaneous Firing of Mouse Midbrain Dopamine Neurons’, *Journal of Neu-*  
 544 *roscience* **27**(3), 645–656.
- 545 Rajakulendran, S., Schorge, S., Kullmann, D. M. and Hanna, M. G. (2007), ‘Episodic ataxia type  
 546 1: A neuronal potassium channelopathy’, *Neurotherapeutics* **4**(2), 258–266.  
 547 **URL:** <https://doi.org/10.1016/j.nurt.2007.01.010>
- 548 Ranjan, R., Logette, E., Marani, M., Herzog, M., Tâche, V., Scantamburlo, E., Buchillier, V. and  
 549 Markram, H. (2019), ‘A Kinetic Map of the Homomeric Voltage-Gated Potassium Channel (Kv)  
 550 Family’, *Frontiers in Cellular Neuroscience* **13**.  
 551 **URL:** <https://www.frontiersin.org/articles/10.3389/fncel.2019.00358/full>
- 552 Ransdell, J. L., Nair, S. S. and Schulz, D. J. (2013), ‘Neurons within the Same Network Inde-  
 553 pendently Achieve Conserved Output by Differentially Balancing Variable Conductance Magni-  
 554 tudes’, *Journal of Neuroscience* **33**(24), 9950–9956.
- 555 Rettig, J., Heinemann, S. H., Wunder, F., Lorra, C., Parcej, D. N., Oliver Dolly, J. and Pongs, O.  
 556 (1994), ‘Inactivation properties of voltage-gated K<sup>+</sup> channels altered by presence of  $\beta$ -subunit’,  
 557 *Nature* **369**(6478), 289–294.  
 558 **URL:** <https://www.nature.com/articles/369289a0>

- 559 Roeper, J., Sewing, S., Zhang, Y., Sommer, T., Wanner, S. G. and Pongs, O. (1998), 'NIP domain  
560 prevents N-type inactivation in voltage-gated potassium channels', *Nature* **391**(6665), 390–393.  
561 **URL:** <https://www.nature.com/articles/34916>
- 562 Ruppertsberg, J. P., Schröter, K. H., Sakmann, B., Stocker, M., Sewing, S. and Pongs, O.  
563 (1990), 'Heteromultimeric channels formed by rat brain potassium-channel proteins', *Nature*  
564 **345**(6275), 535–537.  
565 **URL:** <https://www.nature.com/articles/345535a0>
- 566 Rush, A. M., Dib-Hajj, S. D., Liu, S., Cummins, T. R., Black, J. A. and Waxman, S. G. (2006),  
567 'A single sodium channel mutation produces hyper- or hypoexcitability in different types of  
568 neurons', *Proceedings of the National Academy of Sciences* **103**(21), 8245–8250.  
569 **URL:** <https://www.pnas.org/doi/10.1073/pnas.0602813103>
- 570 Rutecki, P. A. (1992), 'Neuronal excitability: voltage-dependent currents and synaptic transmis-  
571 sion', *Journal of Clinical Neurophysiology: Official Publication of the American Electroen-*  
572 *cephalographic Society* **9**(2), 195–211.
- 573 Saltelli, A. (2002), 'Sensitivity Analysis for Importance Assessment', *Risk Analysis* **22**(3), 579–  
574 590.  
575 **URL:** <https://onlinelibrary.wiley.com/doi/abs/10.1111/0272-4332.00040>
- 576 Saltelli, A. and Annoni, P. (2010), 'How to avoid a perfunctory sensitivity analysis', *Environmental*  
577 *Modelling & Software* **25**(12), 1508–1517.  
578 **URL:** <https://www.sciencedirect.com/science/article/pii/S1364815210001180>
- 579 Scalmani, P., Rusconi, R., Armatura, E., Zara, F., Avanzini, G., Franceschetti, S. and Mantegazza,  
580 M. (2006), 'Effects in Neocortical Neurons of Mutations of the Nav1.2 Na<sup>+</sup> Channel causing Be-  
581 nign Familial Neonatal-Infantile Seizures', *The Journal of Neuroscience* **26**(40), 10100–10109.  
582 **URL:** <https://www.ncbi.nlm.nih.gov/pmc/articles/PMC6674637/>
- 583 Shi, X.-Y., Tomonoh, Y., Wang, W.-Z., Ishii, A., Higurashi, N., Kurahashi, H., Kaneko, S., Hirose,  
584 S. and Epilepsy Genetic Study Group, Japan (2016), 'Efficacy of antiepileptic drugs for the  
585 treatment of Dravet syndrome with different genotypes', *Brain & Development* **38**(1), 40–46.
- 586 Smart, S. L., Lopantsev, V., Zhang, C. L., Robbins, C. A., Wang, H., Chiu, S. Y., Schwartzkroin,  
587 P. A., Messing, A. and Tempel, B. L. (1998), 'Deletion of the KV1.1 Potassium Channel Causes  
588 Epilepsy in Mice', *Neuron* **20**(4), 809–819.  
589 **URL:** <https://www.sciencedirect.com/science/article/pii/S0896627300810181>
- 590 Smith, R. S., Kenny, C. J., Ganesh, V., Jang, A., Borges-Monroy, R., Partlow, J. N., Hill, R. S.,  
591 Shin, T., Chen, A. Y., Doan, R. N., Anttonen, A.-K., Ignatius, J., Medne, L., Bönnemann, C. G.,  
592 Hecht, J. L., Salonen, O., Barkovich, A. J., Poduri, A., Wilke, M., de Wit, M. C. Y., Mancini,  
593 G. M. S., Sztriha, L., Im, K., Amrom, D., Andermann, E., Paetau, R., Lehesjoki, A.-E., Walsh,  
594 C. A. and Lehtinen, M. K. (2018), 'Sodium Channel SCN3A (NaV1.3) Regulation of Human

- 595 Cerebral Cortical Folding and Oral Motor Development', *Neuron* **99**(5), 905–913.e7.  
 596 **URL:** <https://www.sciencedirect.com/science/article/pii/S0896627318306500>
- 597 Soofi, W., Archila, S. and Prinz, A. A. (2012), 'Co-variation of ionic conductances supports phase  
 598 maintenance in stomatogastric neurons', *Journal of Computational Neuroscience* **33**(1), 77–95.  
 599 **URL:** <https://doi.org/10.1007/s10827-011-0375-3>
- 600 Stühmer, W., Ruppersberg, J., Schröter, K., Sakmann, B., Stocker, M., Giese, K., Perschke, A.,  
 601 Baumann, A. and Pongs, O. (1989), 'Molecular basis of functional diversity of voltage-gated  
 602 potassium channels in mammalian brain.', *The EMBO Journal* **8**(11), 3235–3244.  
 603 **URL:** <https://www.embopress.org/doi/abs/10.1002/j.1460-2075.1989.tb08483.x>
- 604 Taylor, A. L., Goaillard, J.-M. and Marder, E. (2009), 'How Multiple Conductances Deter-  
 605 mine Electrophysiological Properties in a Multicompartment Model', *Journal of Neuroscience*  
 606 **29**(17), 5573–5586.
- 607 Tsaour, M.-L., Sheng, M., Lowenstein, D. H., Jan, Y. N. and Jan, L. Y. (1992), 'Differential expres-  
 608 sion of K<sup>+</sup> channel mRNAs in the rat brain and down-regulation in the hippocampus following  
 609 seizures', *Neuron* **8**(6), 1055–1067.  
 610 **URL:** <https://www.sciencedirect.com/science/article/pii/089662739290127Y>
- 611 Van Dyke, D. H., Griggs, R. C., Murphy, M. J. and Goldstein, M. N. (1975), 'Hereditary myokymia  
 612 and periodic ataxia', *Journal of the Neurological Sciences* **25**(1), 109–118.  
 613 **URL:** <https://www.sciencedirect.com/science/article/pii/0022510X75901914>
- 614 Veh, R. W., Lichtinghagen, R., Sewing, S., Wunder, F., Grumbach, I. M. and Pongs, O. (1995),  
 615 'Immunohistochemical Localization of Five Members of the KV1 Channel Subunits: Contrast-  
 616 ing Subcellular Locations and Neuron-specific Co-localizations in Rat Brain', *European Journal*  
 617 *of Neuroscience* **7**(11), 2189–2205.  
 618 **URL:** <https://onlinelibrary.wiley.com/doi/abs/10.1111/j.1460-9568.1995.tb00641.x>
- 619 Verma, P., Kienle, A., Flockerzi, D. and Ramkrishna, D. (2020), 'Computational analysis of a 9D  
 620 model for a small DRG neuron', *Journal of Computational Neuroscience* **48**(4), 429–444.  
 621 **URL:** <https://doi.org/10.1007/s10827-020-00761-6>
- 622 Wang, F. C., Parcej, D. N. and Dolly, J. O. (1999), 'α Subunit compositions of Kv1.1-containing  
 623 K<sup>+</sup> channel subtypes fractionated from rat brain using dendrotoxins', *European Journal of Bio-*  
 624 *chemistry* **263**(1), 230–237.  
 625 **URL:** <https://febs.onlinelibrary.wiley.com/doi/abs/10.1046/j.1432-1327.1999.00493.x>
- 626 Wang, H., Kunkel, D. D., Schwartzkroin, P. A. and Tempel, B. L. (1994), 'Localization of Kv1.1  
 627 and Kv1.2, two K channel proteins, to synaptic terminals, somata, and dendrites in the mouse  
 628 brain', *Journal of Neuroscience* **14**(8), 4588–4599.  
 629 **URL:** <https://www.jneurosci.org/content/14/8/4588>

- 630 Waxman, S. G. (2007), 'Channel, neuronal and clinical function in sodium channelopathies: from  
631 genotype to phenotype', *Nature Neuroscience* **10**(4), 405–409.  
632 **URL:** <https://www.nature.com/articles/nn1857>
- 633 Weber, Y. G., Biskup, S., Helbig, K. L., Von Spiczak, S. and Lerche, H. (2017), 'The role of  
634 genetic testing in epilepsy diagnosis and management', *Expert Review of Molecular Diagnostics*  
635 **17**(8), 739–750.  
636 **URL:** <https://doi.org/10.1080/14737159.2017.1335598>
- 637 Xu, J. and Li, M. (1997), 'Kv $\beta$ 2 Inhibits the Kv $\beta$ 1-mediated Inactivation of K<sup>+</sup> Channels in Trans-  
638 fected Mammalian Cells', *Journal of Biological Chemistry* **272**(18), 11728–11735.  
639 **URL:** <https://www.sciencedirect.com/science/article/pii/S0021925818405091>
- 640 Zhang, C.-L., Messing, A. and Chiu, S. Y. (1999), 'Specific Alteration of Spontaneous GABAergic  
641 Inhibition in Cerebellar Purkinje Cells in Mice Lacking the Potassium Channel Kv1.1', *Journal*  
642 *of Neuroscience* **19**(8), 2852–2864.  
643 **URL:** <https://www.jneurosci.org/content/19/8/2852>
- 644 Zhao, J., Petitjean, D., Haddad, G. A., Batulan, Z. and Blunck, R. (2020), 'A Common Kinetic  
645 Property of Mutations Linked to Episodic Ataxia Type 1 Studied in the Shaker Kv Channel',  
646 *International Journal of Molecular Sciences* **21**(20), 7602.  
647 **URL:** <https://www.mdpi.com/1422-0067/21/20/7602>
- 648 Zhou, L., Zhang, C.-L., Messing, A. and Chiu, S. Y. (1998), 'Temperature-Sensitive Neuromuscu-  
649 lar Transmission in Kv1.1 Null Mice: Role of Potassium Channels under the Myelin Sheath in  
650 Young Nerves', *Journal of Neuroscience* **18**(18), 7200–7215.  
651 **URL:** <https://www.jneurosci.org/content/18/18/7200>
- 652 Zuberi, S. M., Eunson, L. H., Spauschus, A., De Silva, R., Tolmie, J., Wood, N. W., McWilliam,  
653 R. C., Stephenson, J. P. B., Kullmann, D. M. and Hanna, M. G. (1999), 'A novel mutation in the  
654 human voltage-gated potassium channel gene (Kv1.1) associates with episodic ataxia type 1 and  
655 sometimes with partial epilepsy', *Brain* **122**(5), 817–825.  
656 **URL:** <https://doi.org/10.1093/brain/122.5.817>

## Figure/Table/Extended Data Legends

Figure 1: Characterization of firing with AUC and rheobase. (A) The area under the curve (AUC) of the repetitive firing frequency-current (fI) curve. (B) Changes in firing as characterized by  $\Delta$ AUC and  $\Delta$ rheobase occupy 4 quadrants separated by no changes in AUC and rheobase. Representative schematic fI curves in blue with respect to a reference fI curve (black) depict the general changes associated with each quadrant.

Figure 2: Diversity in Neuronal Model Firing. Spike trains (left), frequency-current (fI) curves (right) for Cb stellate (A), RS inhibitory (B), FS (C), RS pyramidal (D), RS inhibitory +K<sub>V</sub>1.1 (E), Cb stellate +K<sub>V</sub>1.1 (F), FS +K<sub>V</sub>1.1 (G), RS pyramidal +K<sub>V</sub>1.1 (H), STN +K<sub>V</sub>1.1 (I), Cb stellate  $\Delta$ K<sub>V</sub>1.1(J), STN  $\Delta$ K<sub>V</sub>1.1(K), and STN (L) neuron models. Black marker on the fI curves indicate the current step at which the spike train occurs. The green marker indicates the current at which firing begins in response to an ascending current ramp, whereas the red marker indicates the current at which firing ceases in response to a descending current ramp.

Figure 3: The Kendall rank correlation (Kendall  $\tau$ ) coefficients between shifts in  $V_{1/2}$  and AUC, slope factor k and AUC as well as current conductances and AUC for each model are shown on the right in (A), (B) and (C) respectively. The relationships between AUC and  $\Delta V_{1/2}$ , slope (k) and conductance (g) for the Kendall  $\tau$  coefficients highlights by the black box are depicted in the middle panel. The fI curves corresponding to one of the models are shown in the left panels.

Figure 4: The Kendall rank correlation (Kendall  $\tau$ ) coefficients between shifts in  $V_{1/2}$  and rheobase, slope factor k and AUC as well as current conductances and rheobase for each model are shown on the right in (A), (B) and (C) respectively. The relationships between rheobase and  $\Delta V_{1/2}$ , slope (k) and conductance (g) for the Kendall  $\tau$  coefficients highlights by the black box are depicted in the middle panel. The fI curves corresponding to one of the models are shown in the left panels.

Figure 5: Effects of episodic ataxia type 1 associated K<sub>V</sub>1.1 mutations on firing. Effects of K<sub>V</sub>1.1 mutations on AUC ( $AUC_{contrast}$ ) and rheobase ( $\Delta$ rheobase) compared to wild type for RS pyramidal +K<sub>V</sub>1.1 (A), RS inhibitory +K<sub>V</sub>1.1 (B), FS +K<sub>V</sub>1.1 (C), Cb stellate (D), Cb stellate +K<sub>V</sub>1.1 (E), Cb stellate  $\Delta$ K<sub>V</sub>1.1(F), STN (G), STN +K<sub>V</sub>1.1 (H) and STN  $\Delta$ K<sub>V</sub>1.1(I) models V174F, F414C, E283K, and V404I mutations are highlighted in color for each model. Pair-wise Kendall rank correlation coefficients (Kendall  $\tau$ ) between the effects of K<sub>V</sub>1.1 mutations on rheobase and on AUC are shown in J and K respectively.



	RS Pyra- midal	RS Inhib- itory	FS	Cb Stellate	Cb Stellate +K <sub>V</sub> 1.1	Cb Stellate $\Delta$ K <sub>V</sub> 1.1	STN	STN +K <sub>V</sub> 1.1	STN $\Delta$ K <sub>V</sub> 1.1
$g_{Na}$	56	10	58	3.4	3.4	3.4	49	49	49
$g_K$	5.4	1.89	3.51	9.0556	8.15	9.0556	57	56.43	57
$g_{K_V1.1}$	0.6	0.21	0.39	—	0.90556	1.50159	—	0.57	0.5
$g_A$	—	—	—	15.0159	15.0159	—	5	5	—
$g_M$	0.075	0.0098	0.075	—	—	—	—	—	—
$g_L$	—	—	—	—	—	—	5	5	5
$g_T$	—	—	—	0.45045	0.45045	0.45045	5	5	5
$g_{Ca,K}$	—	—	—	—	—	—	1	1	1
$g_{Leak}$	0.0205	0.0205	0.038	0.07407	0.07407	0.07407	0.035	0.035	0.035
$\tau_{max,M}$	608	934	502	—	—	—	—	—	—
$C_m$	118.44	119.99	101.71	177.83	177.83	177.83	118.44	118.44	118.44

Table 1: Cell properties and conductances of regular spiking pyramidal neuron (RS Pyramidal), regular spiking inhibitory neuron (RS Inhibitory), fast spiking neuron (FS), cerebellar stellate cell (Cb Stellate), with additional I<sub>K<sub>V</sub>1.1</sub> (Cb Stellate  $\Delta$ K<sub>V</sub>1.1 ) and with I<sub>K<sub>V</sub>1.1</sub> replacement of I<sub>A</sub> (Cb Stellate  $\Delta$ K<sub>V</sub>1.1 ), and subthalamic nucleus neuron (STN), with additional I<sub>K<sub>V</sub>1.1</sub> (STN  $\Delta$ K<sub>V</sub>1.1 ) and with I<sub>K<sub>V</sub>1.1</sub> replacement of I<sub>A</sub> (STN K<sub>V</sub>1.1 ) models. All conductances are given in mS/cm<sup>2</sup>. Capacitances ( $C_m$ ) and  $\tau_{max,M}$  are given in pF and ms respectively.

Extended Data 1: TODO: Caption for code in zip file.

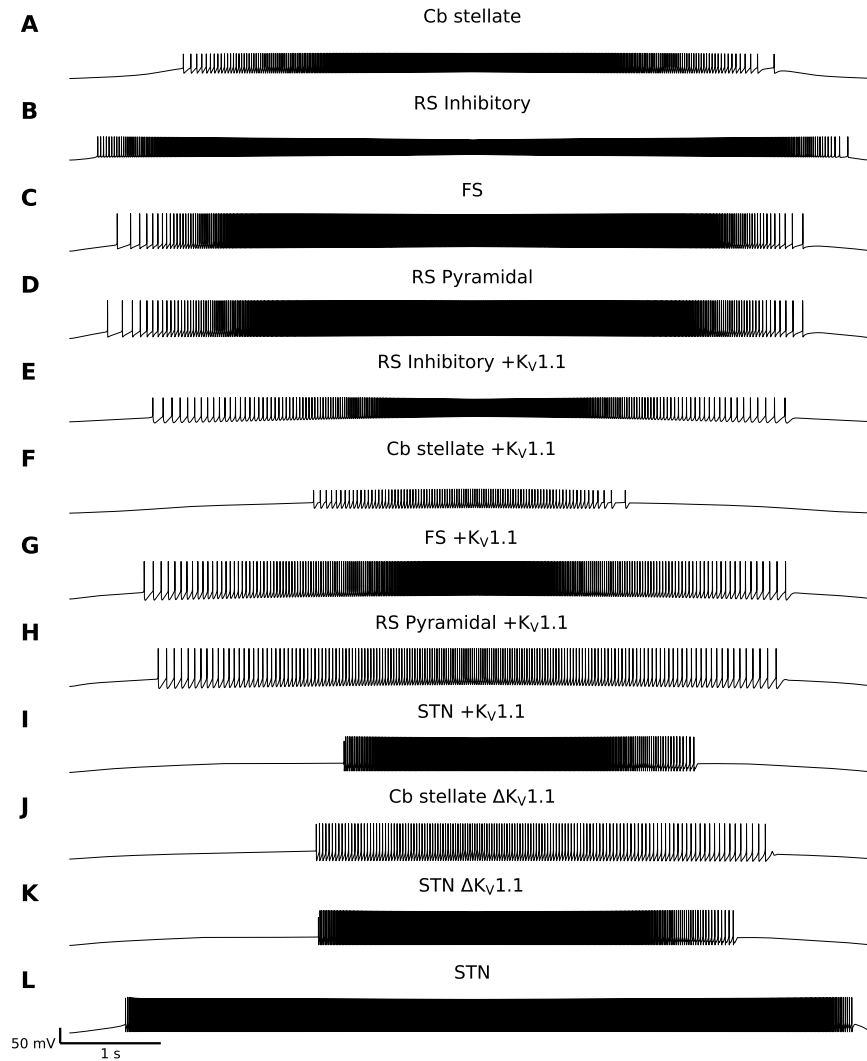


Figure 2-1: Diversity in Neuronal Model Firing Responses to a Current Ramp. Spike trains for Cb stellate (A), RS inhibitory (B), FS (C), RS pyramidal (D), RS inhibitory +K<sub>V</sub>1.1 (E), Cb stellate +K<sub>V</sub>1.1 (F), FS +K<sub>V</sub>1.1 (G), RS pyramidal +K<sub>V</sub>1.1 (H), STN +K<sub>V</sub>1.1 (I), Cb stellate  $\Delta$ K<sub>V</sub>1.1 (J), STN  $\Delta$ K<sub>V</sub>1.1 (K), and STN (L) neuron models in response to a slow ascending current ramp followed by the descending version of the current ramp. The current at which firing begins in response to an ascending current ramp and the current at which firing ceases in response to a descending current ramp are depicted on the frequency current (f) curves in Figure 2 for each model.